Monthly Notices
of the
ROYAL ASTRONOMICAL SOCIETY

MNRAS **449,** 1228–1237 (2015) doi:10.1093/mnras/stv341

INTEGRAL discovery of unusually long broad-band X-ray activity from the Supergiant Fast X-ray Transient IGR J18483−0311

V. Sguera,[1★] L. Sidoli,[2] A. J. Bird[3] and A. Bazzano[4]

[1] *INAF, Istituto di Astrofisica Spaziale e Fisica Cosmica, Via Gobetti 101, I-40129 Bologna, Italy*
[2] *INAF, Istituto di Astrofisica Spaziale e Fisica Cosmica, Via E. Bassini 15, I-20133 Milano, Italy*
[3] *School of Physics and Astronomy, Faculty of Physical Sciences and Engineering, University Southampton, SO17 1BJ Southampton, UK*
[4] *INAF, Istituto di Astrofisica e Planetologia Spaziali, Via Fosso del Cavaliere 100, I-00133 Rome, Italy*

Accepted 2015 February 16. Received 2015 February 16; in original form 2014 December 16

ABSTRACT

We report on a broad-band X-ray study (0.5–250 keV) of the Supergiant Fast X-ray Transient IGR J18483−0311 using archival *INTEGRAL* data and a new targeted *XMM–Newton* observation. Our *INTEGRAL* investigation discovered for the first time an unusually long X-ray activity (3–60 keV) which continuously lasted for at least ∼11 d, i.e. a significant fraction (∼60 per cent) of the entire orbital period, and spanned orbital phases corresponding to both periastron and apastron passages. This prolongated X-ray activity is at odds with the much shorter durations marking outbursts from classical SFXTs especially above 20 keV, as such it represents a departure from their nominal behaviour and it adds a further extreme characteristic to the already extreme SFXT IGR J18483−0311. Our IBIS/ISGRI high energy investigation (100–250 keV) of archival outbursts activity from the source showed that the recently reported hint of a possible hard X-ray tail is not real and it is likely due to noisy background. The new *XMM–Newton* targeted observation did not detect any sign of strong X-ray outburst activity from the source despite being performed close to its periastron passage, on the contrary IGR J18483−0311 was caught during the common intermediate X-ray state with a low-luminosity value of $\sim 3 \times 10^{33}$ erg s^{-1} (0.5–10 keV). We discuss all the reported results in the framework of both spherically symmetric clumpy wind scenario and quasi-spherical settling accretion model.

Key words: X-rays: binaries – X-rays: individual: IGR J18483−0311.

1 INTRODUCTION

The IBIS/ISGRI instrument onboard the *INTEGRAL* observatory, launched in 2002 October, has inaugurated a new era in the study of High-Mass X-ray Binaries (HMXBs) by discovering a peculiar subclass during systematic scans of the Galactic plane: the Supergiant Fast X-ray Transients (SFXTs). SFXTs usually host a neutron star compact object orbiting around a massive and hot OB blue supergiant star as companion donor (Negueruela et al. 2006), in the X-ray band they display a peculiar fast X-ray transient behaviour lasting typically from a few hours to no longer than a few days (Sguera et al. 2005, 2006). Notably the typical dynamic ranges, from X-ray outbursts ($L_x \sim 10^{36}$–10^{37} erg s^{-1}) to the lowest level of X-ray emission, are of the order of 10^3–10^5: SFXTs are among the most extreme and exotic X-ray transients in our Galaxy. This exceptional fast X-ray transient behaviour is at odds with the bright and persistent X-ray emission ($L_x \sim 10^{36}$ erg s^{-1}) characterizing their historical parent population of wind-fed Supergiant High-Mass X-ray Binaries (SGXBs).

Despite the elusive nature which makes their discovery challenging, during the last 9 yr ∼10 firm SFXTs have been reported in the literature (see list in Paizis & Sidoli 2014) plus a similar number of candidates (e.g. Sguera et al. 2013). SFXTs could represent a significant portion of the entire population of HMXBs in our Galaxy, in particular they could constitute a large fraction of HMXBs with supergiant companions (Ducci et al. 2014).

The physical mechanism driving the peculiar X-ray behaviour of SFXTs is far from solved, although several different models have been proposed in the last decade. All invoke a structured and inhomogeneous supergiant stellar wind (the so-called clumpy wind model) and could be broadly divided into two different groups: (i) models involving a neutron star compact object with standard magnetic field values (e.g. 10^{11-12} Gauss) acting as a probe of the clumped supergiant wind properties; the fast X-ray outbursts are assumed to be due to accretion of single and very massive clumps embedded in a much less dense background wind (Sidoli et al. 2007; Walter & Zurita 2007; Negueruela et al. 2008; Ducci, Sidoli

★ E-mail: sguera@iasfbo.inaf.it

& Mereghetti 2009), (ii) models involving a slowly rotating (e.g. ≥1000 s) and highly magnetized neutron star (e.g. $\sim 10^{14-15}$ Gauss) where the accretion of single massive clumps is prevented or allowed by the switching of a magnetic or centrifugal barrier, the conditions for their onset can be modified by even modest variations of the clumpy wind parameters (e.g. density and speed) as expected for example close to the periastron passage (Grebenev & Sunyaev 2007; Bozzo, Falanga & Stella 2008). All such models rapidly became the preferred mechanisms to explain the overall behaviour of SFXTs since the early days of their discovery. However in recent years, new observational findings clearly showed that these models have several shortcomings (e.g. Oskinova, Feldmeier & Kretschmar 2012), and can hardly explain the different X-ray behaviour between SFXTs and their historical parent population of persistent SGXBs and are not able to justify the whole observational phenomenology of SFXTs. In this respect, an interesting step forward has been very recently represented by the novel theoretical development proposed by Shakura, Postnov & Hjalmarsdotter (2013) and Shakura et al. (2012): the model of quasi-spherical settling accretion. Although it was initially proposed to explain the off states observed in slowly rotating X-ray pulsars hosted in HMXBs, it has since been applied to the case of SFXTs (Drave et al. 2013, 2014; Paizis & Sidoli 2014; Shakura et al. 2014). Such a model, which has also the benefit of elegantly explaining the different X-ray behaviour between the persistent SGXBs and the SFXTs, is not mutually exclusive from the clumpy wind scenario but it does not have its main shortcomings and limitations. In this model, the accretion on to the neutron star compact object is mediated through a quasi-static shell of plasma above the magnetosphere, the actual mass accretion rate depends on the ability of the plasma shell to enter the neutron star magnetosphere which in turn depends on the cooling mechanism. The fast flaring events observed from SFXTs are likely generated by a transition from a radiatively inefficient cooling regime (which allows only very low accretion rate on to the neutron star) to a much more efficient Compton cooling regime (which allows for a brief period a much higher accretion rate). This transition occurs when the X-ray luminosity decreases/increases below/above the critical value of $\sim 3 \times 10^{35}$ erg s^{-1} (Shakura et al. 2012, 2013).

IGR J18483−0311 is among the most studied SFXTs. It was discovered in outburst with *INTEGRAL* in 2003 (Chernyakova, Lutovinov & Capitanio 2003) during observations of the Galactic centre region. Since then several other X-ray outbursts were observed by *INTEGRAL* showing hard X-ray fluxes up to $\sim 10^{-9}$ erg cm^{-2} s^{-1} and typical durations from ∼0.2 to 3 d (Sguera et al. 2007; Ducci et al. 2013). The optical counterpart has been identified with a massive B0.5–B1 supergiant star located at a distance in the range 2.8–4 kpc (Rahoui & Chaty 2008; Torrejon et al. 2010). The X-ray emission shows two periodicities: the longer one (at ∼18.5 d) is interpreted as due to the orbital period (Levine & Corbet 2006; Sguera et al. 2007) while the shorter one (at ∼21 s) was discovered with the soft X-ray monitor JEM-X onboard *INTEGRAL* (Sguera et al. 2007) and it is interpreted as due to the spin of the neutron star compact object. Giunta et al. (2009) confirmed the detection of X-ray pulsations through *XMM–Newton* data.[1] The lowest X-ray luminosity states have been measured at $\sim 1.3 \times 10^{33}$ erg s^{-1} in the soft X-rays (Giunta et al. 2009; Sguera et al. 2010) and at $\sim 1.3 \times 10^{34}$ erg s^{-1} in the hard X-rays (Sguera et al. 2010), by assuming a distance of 3 kpc. Monitoring of the soft X-ray emission over an entire orbital period has been performed in 2009 with *Swift*/XRT (Romano et al. 2010). Sguera et al. (2010) reported on a possible cyclotron feature in the *XMM–Newton* spectrum which would imply a neutron star magnetic field of the order of 3×10^{11} Gauss. From a broad-band X-ray spectral study of IGR J18483−0311 in outburst, Ducci et al. (2013) reported the hint of a possible hard X-ray tail at energies above ∼80 keV and extending up to ∼250 keV.

Here, we report new results on the SFXT IGR J18483−0311 both below and above 10 keV as obtained from a new targeted *XMM–Newton* observation and archival *INTEGRAL* data, respectively.

2 DATA ANALYSIS

2.1 *INTEGRAL*

We have used data collected with the gamma-ray imager IBIS/ISGRI (Lebrun et al. 2003; Ubertini et al. 2003) onboard the *INTEGRAL* satellite (Winkler et al. 2003) from the end of 2003 February to the end of 2010 December. In particular, the IBIS/ISGRI data set consists of 4735 pointings or Science Windows (ScWs, typical duration 2000 s) where IGR J18483−0311 was within 12° from the centre of the IBIS/ISGRI field of view (FoV) with an exposure greater than at least 500 s. We applied a 12° limit because the off-axis response of IBIS/ISGRI is not well modelled at large off-axis angles and in combination with the telescope dithering (or the movement of the source within the FoV) it may introduce systematic errors in the measurement of the source fluxes. IBIS/ISGRI images for each ScW were generated in the energy band 18–60 keV and count rates at the position of the source were then extracted from all individual images to produce the 18–60 keV long-term light curve on the ScW time-scale.

The X-ray monitor JEM-X (Lund et al. 2003) on board the *INTEGRAL* has an ∼6° diameter fully coded FoV and performs observations simultaneously with IBIS/ISGRI (fully coded FoV of 9° × 9°) in the energy band 3–35 keV. Images from JEM-X (3–10 and 10–20 keV) were created for all the ScWs during which the source was in the IBIS/ISGRI FoV from revolution number 906 to 919 (see Section 3.1.1), count rates at the position of the source were then extracted from all individual images to produce the 3–10 keV long-term light curve on the ScW time-scale.

The data reduction was carried out with the release 9.0 of the Offline Scientific Analysis (OSA) software. Through the paper, the spectral analysis was performed using XSPEC version 12.8.2 and, unless stated otherwise, errors are quoted at the 90 per cent confidence level for one single parameter of interest.

2.2 *XMM–Newton*

For the present study, we analysed a new targeted *XMM–Newton* observation of IGR J18483−0311 performed on 2013 April 18. Data reduction was carried out using the latest Science Analysis System (SAS v13.5) and following standard procedures. The EPIC-mos (Turner et al. 2001) and EPIC-pn (Struder et al. 2001) cameras were operated in Full Frame mode. The SAS tasks EPCHAIN and EMCHAIN were applied to produce calibrated event lists for both detectors, respectively.

The total exposure was about 58 ks, however after subtraction of high flaring background period the net exposure turned out to be 36.2 ks for the EPIC-pn. The source counts were extracted from a circular region of 25 arcsec in radius, while counts from the background were extracted from a source-free region in the same CCD. The redistribution and ancillary matrices were generated using the

[1] This spin period has been recently called into question by Ducci et al. (2013).

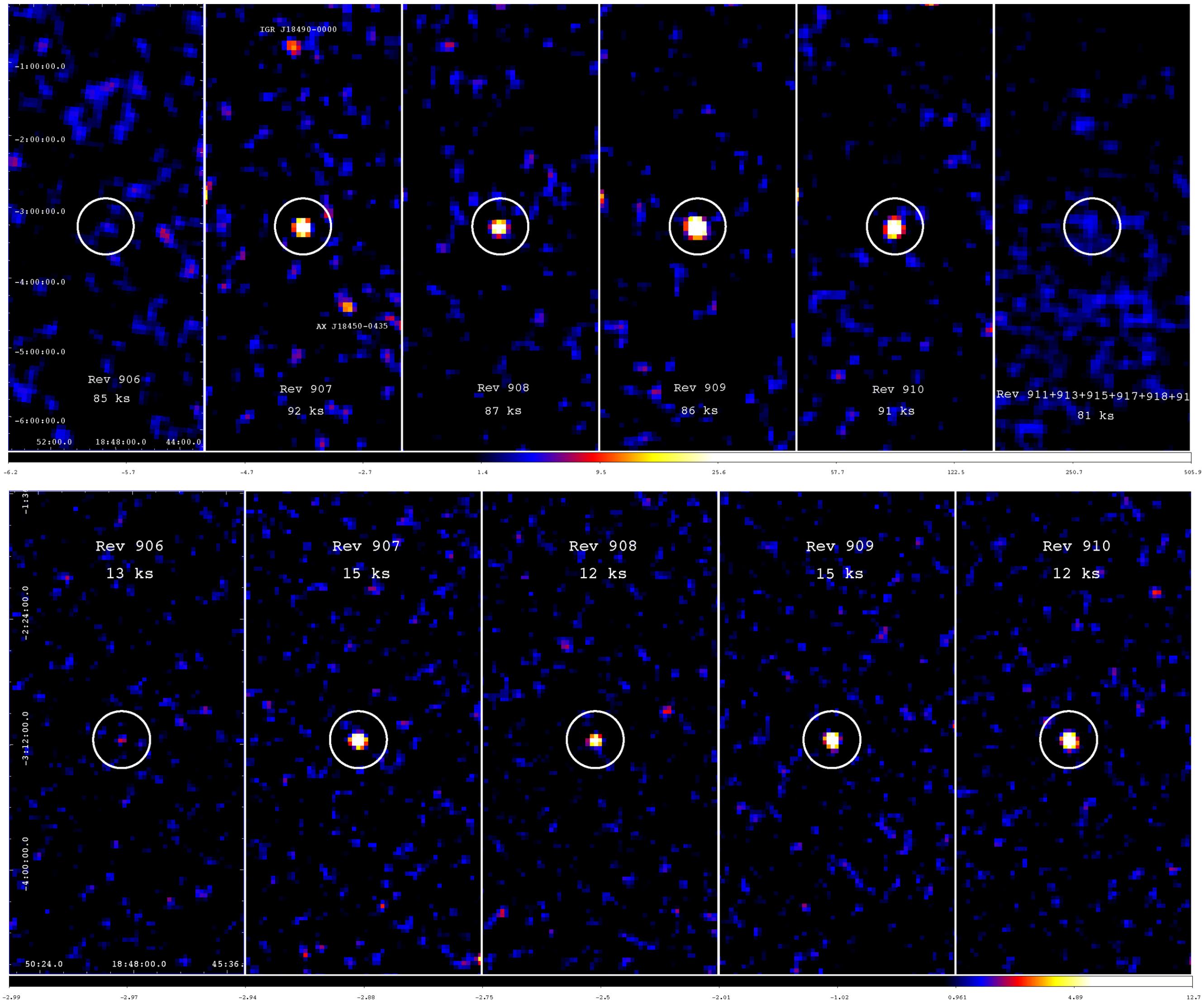

Figure 1. IBIS/ISGRI revolution image sequence (18–60 keV, top) and *INTEGRAL*/JEM-X revolution image sequence (3–10 keV, bottom) of the outburst X-ray activity detected from IGR J18483−0311 (encircled).

SAS tasks ARFGEN and RMFGEN. Spectra and light curves were selected from single and double events only (pattern from 0 to 4) for the EPIC-pn while for both mos cameras patterns from 0 to 12 were selected. The source net count rates for the three cameras are 0.278 ± 0.002 (pn), 0.069 ± 0.001 (mos1) and 0.091 ± 0.001 (mos2). The pn has the higher net count rate, hence we decided to consider only data from this instrument in the following. Indeed, the spectroscopy with both the mos cameras does not provide any improvement with respect to the analysis of the pn spectrum alone. Also, the source is too faint for a meaningful spectral analysis with the Reflection Grating Spectrometers onboard *XMM–Newton*. The presence of possible pile up was checked using the task EPATPLOT, however no significant pile up fraction was found neither in the pn nor in the two mos cameras. Background subtracted light curves were generated from event files to which a barycentric correction has been applied using the SAS task BARYCEN. The background count rate was then subtracted to the light curve with the task EPICLCCORR. In order to guarantee the application of the χ^2 statistics, data were grouped to a minimum of 25 counts per bin.

3 *INTEGRAL* RESULTS

3.1 IBIS/ISGRI

3.1.1 *Unusually long outburst activity*

From an analysis at the ScW level of all the deconvolved IBIS/ISGRI shadowgrams, we report on a newly discovered and particularly long hard X-ray outburst activity from the SFXT IGR J18483−0311. During the period from 2010 March 15 10:30 UTC to 2010 March 30 02:00 UTC, corresponding to five consecutive *INTEGRAL* spacecraft revolutions from number 906 to 910, the source was well covered by IBIS/ISGRI observations being in its FoV for a significant amount of time. As we can clearly see in Fig. 1 (top), IGR J18483−0311 was not detected in the 18–60 keV significance image of revolution 906 despite being observed for a total on-source time of 85 ks. On the contrary, it was significantly detected in all the subsequent four revolutions (from number 907 to 910) with 18–60 keV significance value (exposure) of 15.6σ (92 ks), 13σ (87 ks), 24.5σ (86 ks) and 22.3σ (91 ks), respectively.

Table 1. Characteristics of the X-ray outburst from IGR J18483−0311 analysed in this paper. Average fluxes and significance values are provided in the energy band 18–60 keV for IBIS/ISGRI and 3–10 keV for JEM-X.

Orbital revolution	IBIS exp (ks)	IBIS sig	IBIS flux (mCrab)	JEM-X exp (ks)	JEM-X sig	JEM-X flux (mCrab)
906	85		$<0.9^{a}$	13	2.5σ	2.3
907	92	15.6σ	7.3	15	11σ	10.3
908	87	13.0σ	6.8	12	8σ	9.2
909	86	24.5σ	11.3	15	12σ	11.2
910	91	22.0σ	10.6	12	11σ	11.3
911–919	81		$<1^{a}$	0		

Note. $^{a}2\sigma$ upper limit

Unfortunately the IBIS/ISGRI temporal coverage of the source was much poorer during all the subsequent revolutions (i.e. 911, 913, 915, 917, 918, 919) being ∼14 ks exposure in each revolution. No significant detection was obtained in any of these single revolutions, however since such non-detections could have been largely hampered by the significantly lower exposure times (if compared to those during previous revolutions) we summed all the revolutions up to obtain a 18–60 keV significance image with a relevant total exposure time on-source of ∼81 ks. As we can clearly see in Fig. 1 (top), IGR J18483−0311 was not significantly detected and so we can safely state that the source was not active anymore from revolution 910 on. The start time of the outburst activity can be well constrained at 2010 March 19 UTC 05:13 (∼55274.2 MJD), unfortunately its end time cannot be constrained as well because of the much poorer and sparser IBIS/ISGRI temporal coverage of the outburst towards its end of activity. Despite this drawback, a very conservative end time can be assumed as the finish of the last revolution (i.e. 910) during which there was highly significant detection (2010 March 29 UTC 21:00). This implies a conservative lower limit on the outburst duration of the order of ∼10.6 d. Table 1 reports the main characteristics of such X-ray outburst activity as investigated by *INTEGRAL* from revolution 906 to 919.

Fig. 2 (top) shows the IBIS/ISGRI 18–60 keV light curve on ScW time-scales (bin time of ∼2000 s) covering revolutions from 906 to 910, the dotted black line represents the instrumental 2σ upper limit at the ScW level (∼10 mCrab or 1.3×10^{-10} erg cm^{-2} s^{-1}). Clearly, during the entire rev 906 the source was undetected its flux consistent being with the zero value and well below the instrumental sensitivity of IBIS/ISGRI. Conversely, in rev 907 the source suddenly turned on and flared up reaching a peak flux of 54 ± 7 mCrab or $(7.0 \pm 0.9) \times 10^{-10}$ erg cm^{-2} s^{-1} in only ∼6 h, the corresponding luminosity is ∼7.5×10^{35} erg s^{-1} (at 3 kpc distance). The dynamic range of the source from the 2σ upper limit in rev 906 (0.9 mCrab) to the peak-flux is 60. In all the subsequent revolutions from 908 to 910, the source was active and variable up to a factor of ∼5 on ScW time-scales. To investigate possible enhancements of the variability factor due to more structured and stronger flares on much shorter time-scale, we produced the 18–60 keV IBIS/ISGRI light curve with a finer bin time of 500 s, however no significantly stronger flares where evident in the light curve.

If we follow Sguera et al. (2007) and measure the source phase from the epoch of the brightest outburst observed with *INTEGRAL* at MJD 53844.1 (phase 0, periastron) by considering the refined orbital period value of 18.545 ± 0.003 (Levine et al. 2011), then the hard X-ray outburst activity spans orbital phases from ∼0.91 to ∼0.45 (i.e. from close periastron approach to close apastron approach) and lasted for ∼60 per cent of the entire orbital period.

We extracted the IBIS/ISGRI spectrum of the source from its entire outburst activity (revolution 907–910, 38σ detection, 355 ks exposure on-source). The 20–60 keV spectrum is well fitted by a simple power-law model with $\Gamma = 2.8 \pm 0.2$ ($\chi^2_{\nu} = 1.09$, 14 d.o.f.), the average 18–60 keV (60–100 keV) flux is equal to 2.1×10^{-10} erg cm^{-2} s^{-1} (3.5×10^{-11} erg cm^{-2} s^{-1}) which translates into a X-ray luminosity of 2.3×10^{35} erg s^{-1} (3.8×10^{34} erg s^{-1}) at 3 kpc distance.

For the sake of completeness, we note that Ducci et al. (2013) recently reported on several outbursts from IGR J18483−0311 as detected with *INTEGRAL* in the energy band 18–50 keV. In their work, the authors mention the detection of the source during each single revolution 907, 909 and 910. However, such detections were considered as corresponding to three different and distinct outburst activities lasting about 0.5, 1.6 and 0.6 d, respectively. More importantly, no detection of the source in revolution 908 was reported by Ducci et al (2013). We cannot fully establish the origin of the latter difference in results since Ducci et al (2013) did not provide some essential information, specifically the significance threshold used for outburst recognition at revolution level. Without this, or the *INTEGRAL* significance values (both IBIS/ISGRI and JEM-X) pertaining to their detection of the outburst activity from each single revolutions 907 to 910, we cannot explain why they did not detect the signal in revolution 908. However, we note that revolution 908 is also our lowest flux/significance positive detection in this sequence, so it is possible that it was marginally below their detection threshold while the other revolutions were not.

3.1.2 *Investigation of the possible hard X-ray tail*

Ducci et al. (2013) recently reported the presence of a possible hard excess at energies above ∼80 keV (and possibly extending up to ∼250 keV) in the average 3–250 keV broad-band JEM-X+ISGRI X-ray spectrum of IGR J18483−0311 in outburst. According to the F-test, the putative hard X-ray tail was significant at less than 3σ level (Ducci et al. 2013). It is important to point out that to date no detection of SFXTs at energies above ∼100 keV has never been reported in the literature, both from imaging and spectral analysis. As a consequence, according to the hint reported by Ducci et al. (2013), IGR J18483−0311 could possibly be the SFXT with the hardest X-ray spectrum known, with very important implications for the theoretical models usually invoked to explain the physical reasons behind the X-ray behaviour of SFXTs. Given the importance of such a point, we performed an imaging analysis in the energy band 100–250 keV to investigate a possible significant detection of the source which could eventually confirm or not the real nature of

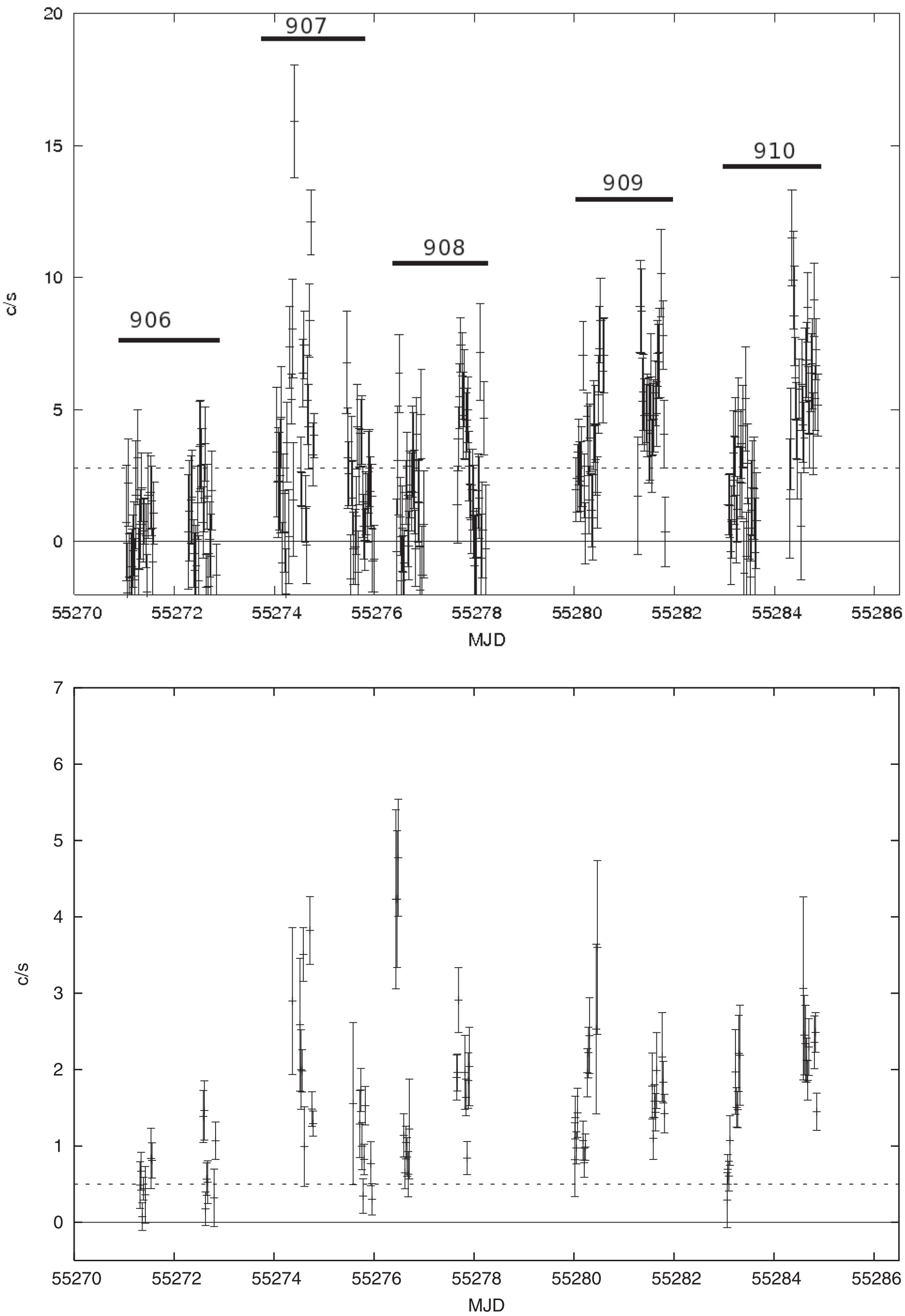

Figure 2. IBIS/ISGRI light curve (18–60 keV, top) and *INTEGRAL*/JEM-X light curve (3–10 keV, bottom) of the X-ray outburst from IGR J18483−0311. The bin time is 2000 s in both light curves and the dotted black line represents the instrumental 2σ upper limit at the ScW level.

the putative hard X-ray tail. Following all the information reported in Table 1 and section 2.1 in Ducci et al. (2013), we produced a 100–250 keV mosaic significance image by using all the ScWs during which the source was significantly detected in outburst in the range 18–50 keV (total exposure of ∼370 ks). IGR J18483−0311 was not significantly detected, with the highest significance value (at pixel level) equal to 2.4σ. We inferred a 100–250 keV 3σ upper limit of ∼5 mCrab or 4.3×10^{-11} erg cm^{-2} s^{-1}. The 100–250 keV mosaic image (see Fig. 3) shows that the sky region is clearly characterized by many noisy pixels and/or structures (due to fluctuations of the background) which have significance values in the range ∼(2–4)σ. We conclude that the putative hard X-ray excess reported by Ducci et al. (2013) is not real and it is very likely due to noisy background.

3.2 JEM-X

Fig. 1 (bottom) shows the 3–10 keV JEM-X significance image sequence from revolution 906 to 910. Because of the much smaller JEM-X FoV compared to the IBIS/ISGRI one, the source was inside the JEM-X fully coded FoV during a much smaller number of ScWs and with much lower exposure time. In particular, the source was never inside the JEM-X fully coded FoV during all the revolutions

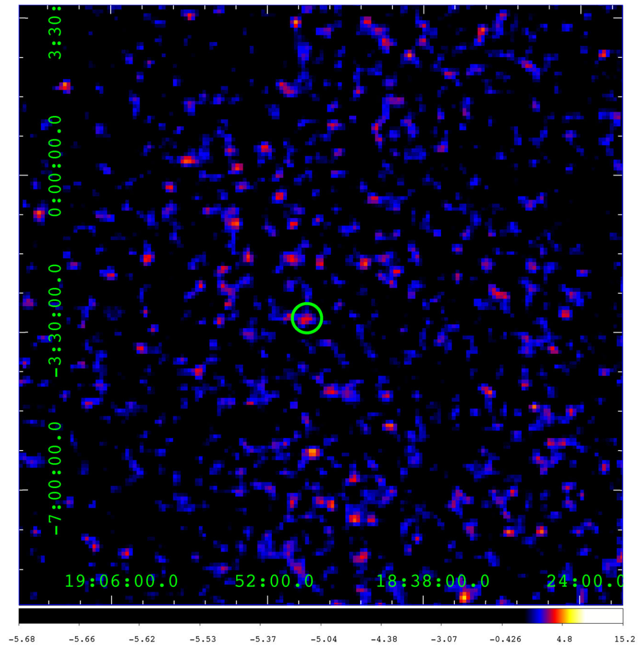

Figure 3. IBIS/ISGRI mosaic significance image (100–250 keV). The circle marks the position of the SFXT IGR J18483−0311.

after number 910. IGR J18483−0311 was barely detected at $\sim 2.5\sigma$ level in the 3–10 keV significance image of revolution 906 (13 ks exposure time), on the contrary it was significantly detected in all the subsequent four revolutions (from number 907 to 910) with 3–10 keV significance values (exposures) of $\sim 11\sigma$ (15 ks), 8σ (12 ks), 12σ (15 ks) and 11σ (12 ks), respectively. It is worth pointing out that the source was significantly detected in the higher energy band 10–20 keV as well, with significance values of 8σ, 5.5σ, 8.5σ and 8σ, respectively.

Fig. 2 (bottom) shows the 3–10 keV JEM-X light curve on ScW time-scales (bin time of ∼2000 s) covering revolutions from 906 to 910, the dotted black line represents the instrumental 2σ upper limit at the ScW level (∼2 mCrab or 2×10^{-11} erg cm^{-2} s^{-1}). During the entire revolution 906, the source flux value was at the limit of the instrumental sensitivity of JEM-X. Conversely in revolution 907, the source suddenly turned on and reached the highest peak flux of 9 ± 3 mCrab (($2.8 \pm 0.5) \times 10^{-10}$ erg cm^{-2} s^{-1}) in revolution 908 (corresponding to a luminosity of $\sim 3 \times 10^{35}$ erg s^{-1} at 3 kpc distance). The dynamic range from the 2σ upper limit in revolution 906 to the peak-flux is about 15 while when active the source was variable by a factor of ∼6 on ScW time-scales. Such JEM-X results clearly confirm that the SFXT IGR J18483−0311 displayed an unusually long X-ray activity not only above 20 keV but also at lower energies in the softer X-ray band.

We extracted the JEM-X spectrum of the source from its entire outburst activity (revolution 907–910, 21σ detection, 55 ks exposure on-source). The 3–20 keV spectrum is reasonably fitted ($\chi^2_\nu = 1.8$, 29 d.o.f.) by an absorbed power-law model with photon index $\Gamma = 1.6 \pm 0.2$ and intrinsic absorption $N_H = (6.8^{+5.1}_{-4.4}) \times 10^{22}$ cm^{-2} in addition to the Galactic one along the line of sight ($\sim 1.6 \times 10^{22}$ cm^{-2}). The average 3–10 keV (10–20 keV) flux is equal to 1.9×10^{-10} erg cm^{-2} s^{-1} (2.2×10^{-10} erg cm^{-2} s^{-1}) which translates into a X-ray luminosity of $\sim 2 \times 10^{35}$ erg s^{-1} (2.4×10^{35} erg s^{-1}) at 3 kpc distance.

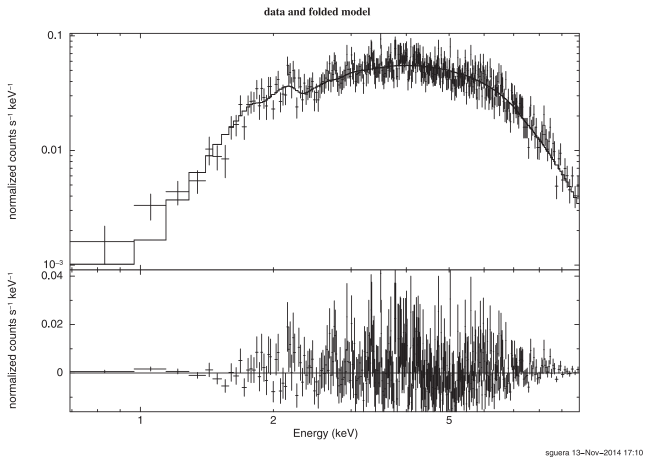

Figure 4. EPIC-pn spectrum of IGR J18483−0311 best fit with an absorbed blackbody.

4 *XMM–Newton* RESULTS

If we follow Sguera et al. (2007) and measure the source phase from the epoch of the brightest outburst observed with *INTEGRAL* at MJD 53844.1 (phase 0, periastron) by considering the refined orbital period value of 18.545 ± 0.003 (Levine et al. 2011), then the *XMM–Newton* observation took place at orbital phase in the range 0.76–0.80, i.e. during the approach to periastron passage.

4.1 Spectral analysis

The average 0.5–10 keV EPIC-pn spectrum was first fitted with an absorbed power-law model ($\chi^2_\nu = 1.11$, 349 d.o.f.) whose parameter values are intrinsic $N_H = 3.7^{+0.3}_{-0.3} \times 10^{22}$ cm^{-2} (in addition to the Galactic one of 1.6×10^{22} cm^{-2}) and $\Gamma = 1.56 \pm 0.08$. The best fit was obtained with an absorbed thermal blackbody ($\chi^2_\nu = 1.01$, 349 d.o.f., see Fig. 4) which yielded spectral parameters values of intrinsic $N_H = 0.98^{+0.16}_{-0.16} \times 10^{22}$ cm^{-2} and $kT = 1.71^{+0.04}_{-0.04}$ keV. We note that the intrinsic N_H value is compatible within the errors with the previous *XMM–Newton* measurement ($N_H = 1.5^{+0.6}_{-0.7} \times 10^{22}$ cm^{-2}; Sguera et al. 2010), on the contrary the blackbody temperature measurement is higher with respect to the previous one ($kT = 1.35^{+0.08}_{-0.08}$ keV). This latter difference could be likely explained in terms of harder-when-brighter spectral X-ray behaviour (as well known in other SFXTs and HMXBs) since in the present *XMM–Newton* observation the flux of the source is higher by a factor of 4 with respect to that during the previous observation (Sguera et al. 2010). The temperature kT resulted in a radius of the emitting blackbody region equal to ∼0.13 km, i.e. consistent with a small portion of the neutron star surface such as its polar cap region. The unabsorbed (intrinsic) 0.5–10 keV flux was 3.8×10^{-12} erg cm^{-2} s^{-1} (3.2×10^{-12} erg cm^{-2} s^{-1}) which translates into a X-ray luminosity of 4.1×10^{33} erg s^{-1} (3.4×10^{33} erg s^{-1}) by assuming a distance of 3 kpc.

4.2 Timing analysis

Fig. 5 shows the EPIC-pn background-subtracted light curve in the energy range 0.5–10 keV (bin time 200 s). It is evident that the source displayed variability on few minutes time-scale by a factor of ∼15. Flickering activity occurred sporadically, following time intervals of lower X-ray emission. In Fig. 6, we report the light curves in the softer (0.5–2 keV) and harder (2–10 keV) X-ray

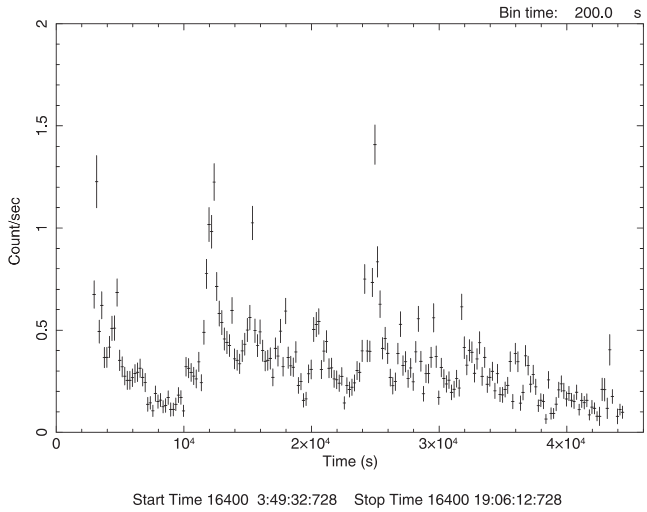

Figure 5. EPIC-pn light curve of IGR J18483−0311 (0.5–10 keV).

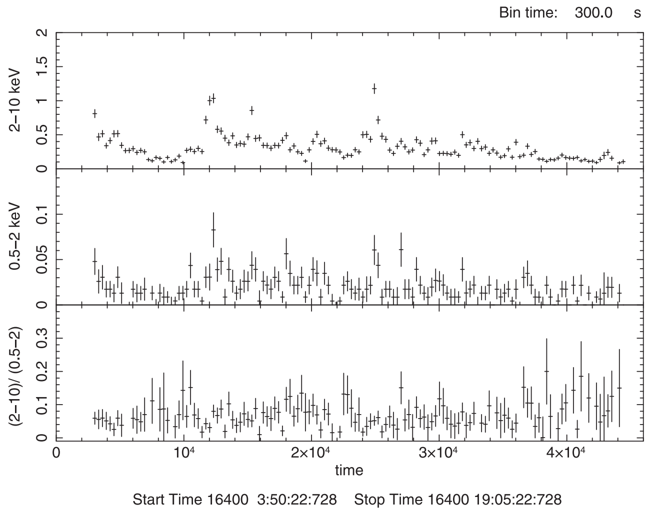

Figure 6. EPIC-pn light curves of IGR J18483−0311 in the energy bands 2–10 keV (top) and 0.5–2 keV (middle). The bottom panel shows the hardness ratio light curve at the same resolution.

bands, in particular the lower panel shows the hardness ratio which clearly indicates that there is no appreciable and significant spectral variation.

We searched for the ∼21 s spin period of the neutron star hosted in IGRJ18483−0311 (Sguera et al. 2007; Giunta et al. 2009). We applied the Solar system barycenter correction to the photon arrival times with the SAS task BARYCEN. Unfortunately, due to the particularly weak signal and low source flux, the production of finely binned light curves (e.g. 1 s, 4 s) resulted in flux values consistent with zero in a lot of the data points in the light curve, preventing a proper and thorough testing of the ∼21 s periodicity. Consecutively, barycentred light curves were extracted with larger time resolution of 8 and 10 s in several energy bands (e.g. 0.5–10, 2–10, 0.5–5, 5–10 keV) and tested for periodicities via the Lomb–Scargle method by means of the fast implementation of Press & Rybicki (1989) and Scargle (1982). Periodicities were searched in the frequency range from 0.000 047 Hz (after which the sensitivity is reduced due to the finite length of the light curves) to 0.06 or 0.05 Hz (corresponding to the Nyquist frequency of the data set), however the intrinsic uncertainties of the light-curve data points resulted in a noise-dominated periodogram without any significant and unambiguous evidence for coherent modulation. Since the Lomb–Scargle method is generally preferred for data set with gaps and unequal sampling (which is not the case of the present *XMM–Newton* observation), after barycentric correction of the photon arrival times in the original event lists we performed a fast Fourier transform analysis. A power spectrum was produced covering the frequency interval as above, however no significant evidence for a peak was found as well. The fractional amplitude to which we are sensitive can be calculated according to Luna & Sokoloski (2007) and it was found that we are sensitive to oscillations with fractional amplitudes of ∼8 per cent (0.5–10 keV). As a subsequent step, we performed an epoch folding analysis. Periodicities were searched for in a small frequency window centred at the putative period of 21 s. While a large value of χ^2 would represent a robust indication of a periodic modulation, again no peak with a significantly high value of χ^2 was found. We note that the strongest peak ($\chi^2 = 36.2$, 7 d.o.f.) in the χ^2 versus $P_{\rm trial}$ plot corresponded to a best period of ∼21.03 s, but was statistically significant at only ∼3σ level (corrected for the number of trial periods, 150).

5 DISCUSSION AND SUMMARY

We presented a broad-band X-ray study (0.5–250 keV) of the SFXT IGR J18483−0311 using archival *INTEGRAL* data and a new targeted *XMM–Newton* observation.

Our *INTEGRAL* investigation discovered for the first time a particularly long X-ray activity (3–60 keV) which continuously lasted for at least ∼11 d, i.e. a very significant fraction (∼60 per cent) of the entire orbital period. This characteristic is at odds with the much shorter durations marking outbursts from classical SFXTs especially above 20 keV both in term of absolute time (typically from few hours to very few days) and fraction of the orbital period (typically ≤ 20 per cent). It is worth pointing out that previous works (Sguera et al. 2007; Ducci et al. 2013) already reported on some X-ray outbursts from the SFXT IGR J18483−0311 lasting a few days. As useful example, Fig. 7 shows the IBIS/ISGRI light curves of the two previously discovered and longest outbursts having duration in the range 2–3 d (see details in Sguera et al. 2007). Remarkably, the newly discovered X-ray activity reported in this work lasted significantly longer (at least ∼11 d) and this adds a further extreme characteristic to the already extreme SFXT IGR J18483−0311. For the sake of completeness, we note that the source IGR J11215−5952 is the only other SFXT known to be also characterized by X-ray outburst activity with a similarly long duration of ∼6–8 d (Romano et al. 2009). However, as recently highlighted by Lorenzo et al. (2014), IGR J11215−5952 is a peculiar SFXT with very eccentric and unusually long orbital period of ∼165 d, such characteristics (as well as its strictly recurrent X-ray behaviour and its position in the Corbet diagram) are akin to those of transient Be HMXBs. Contrarily to other classical SFXTs, during its unusually long X-ray activity IGR J18483−0311 was not characterized by fast/strong X-ray flares but it rather displayed an enhanced X-ray flux moderately variable by a factor of ∼5 both in the hard and soft X-ray bands. At the peak, the 18–60 keV (3–10 keV) luminosity was equal to 7.5×10^{35} erg s^{-1} (3×10^{35} erg s^{-1}) i.e. the source was underluminous by a factor of a few relative to its typical outbursts L_x of the order of ∼10^{36} erg s^{-1} (Sguera et al. 2007). The particularly long X-ray activity detected by *INTEGRAL* lasted for a significant fraction (∼60 per cent) of the entire ∼18 d orbital period, spanning from orbital phase ∼0.91 (very close to periastron approach at 0 phase) to ∼0.45 (very close to apastron approach at 0.5 phase). We note

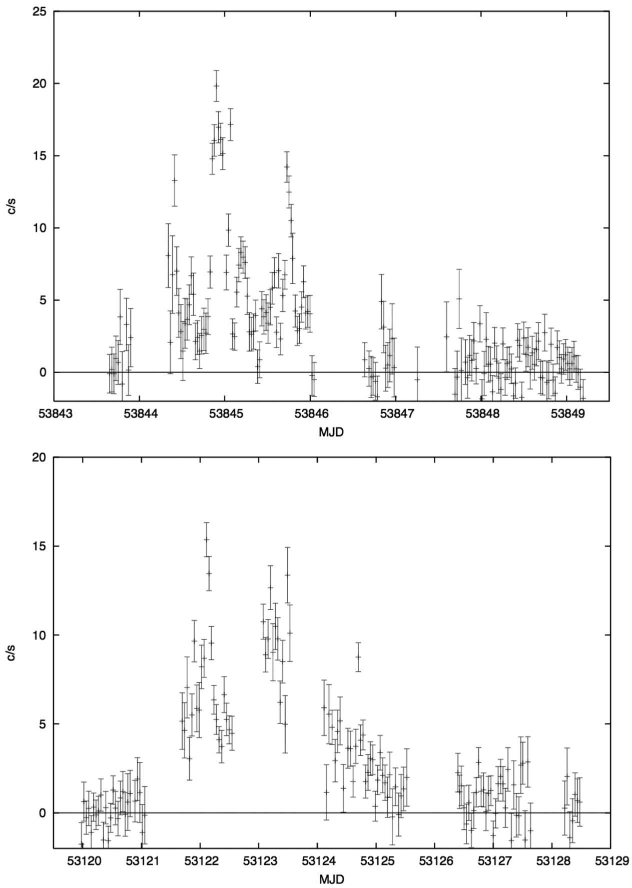

Figure 7. IBIS/ISGRI light curves (18–60 keV) on ScW time-scales (2000 s) of the two longest previously reported X-ray outbursts from IGR J18483−0311.

that previous *INTEGRAL* and *XMM–Newton* investigations around apastron (Sguera et al. 2007, 2010) showed that the source was predominantly undetected at hard X-rays ($L_x < 10^{34}$ erg s^{-1}) and very weak at soft X-rays ($L_x \sim 1.3 \times 10^{33}$ erg s^{-1}). On the contrary the present study reports for the first time relevant X-ray activity during apastron, with X-ray luminosity values more than two orders of magnitude greater with respect to previous measurements both above and below 10 keV. From IBIS/ISGRI and JEM-X analysis, the X-ray spectral shape was identical to that of many other X-ray outbursts already reported in the literature (Sguera et al. 2007; Ducci et al. 2013).

From a new *XMM–Newton* targeted observation, we reported the spectral and temporal properties of the source. Although the observation took place at periastron approach, IGR J18483−0311 was detected at low X-ray luminosity ($\sim 4 \times 10^{33}$ erg s^{-1}, 0.5–10 keV) showing variability by a factor of ∼15 on few minutes time-scale. This kind of behaviour at low L_x has already been observed in other SFXTs (e.g. Bozzo et al. 2010; Sidoli, Esposito & Ducci 2010), it is well known that SFXTs spend the great majority of the time in this so-called intermediate X-ray state (Sidoli et al. 2008) with typical hard X-ray spectra ($\Gamma \sim 1$–2) as result of accretion of material at a much lower rate than that during the bright X-ray outbursts. The hard X-ray spectrum and the low X-ray flux measured by *XMM–Newton* are compatible with this intermediate intensity state scenario. The EPIC-pn spectrum is best fitted by an absorbed blackbody, in particular we note that, contrarily to Sguera et al. (2010), no emission line feature at ∼3.3 keV was evident in the spectrum of the present new *XMM–Newton* observation. Such a line was previously interpreted by Sguera et al. (2010) in term of cyclotron emission feature following the theoretical framework of Nelson, Salpeter & Wasserman (1993) and Nelson et al. (1995), and implies a magnetic field value of about 4×10^{11} G with very important implications on theoretical models. In the light of the newly reported results, the real nature of the putative cyclotron line is called into question and it should be treated with caution. However, we note that according to the theoretical framework of Nelson et al. (1993, 1995) this kind of cyclotron line, if present, becomes detectable only during the lowest X-ray luminosity state of transient HMXBs when their X-ray continuum is the weakest possible. Unfortunately during the present new *XMM–Newton* observation (around periastron passage), the X-ray luminosity of the source was higher by a factor of 4 with respect to that during which the putative line was previously detected (around apastron passage) at the lowest ever measured X-ray luminosity (Sguera et al. 2010). It is likely that the line (especially if weak) was not detectable in the present new *XMM–Newton* observation because it was drowned out by the brighter continuum. Only detailed studies performed at the similarly lowest X-ray luminosity states (achievable only during the apastron passage) can draw a definitive judgement on the nature of the putative line. The EPIC-pn light curves were searched for the ∼21 s spin period of the neutron star hosted in IGR J18483−0311. No significant periodicity was found by performing a Lomb–Scargle and fast Fourier transform analysis and we inferred a fractional amplitude to which the *XMM–Newton* observation is sensitive equal to ∼8 per cent. By performing an epoch folding analysis, the strongest peak in the χ^2 versus $P_{\rm trial}$ plot corresponded to a best period of ∼21.03 s, however it was statistically significant at only $\sim 3\sigma$ level. We caution that the poor statistical quality of the data did not permit us to obtain meaningful high time resolution light curves (e.g. 1 s or 4 s bin time) which are required for a detailed timing analysis. In addition, we note that the measured pulsed fraction reported by Giunta et al. (2009) in a similar energy band and at similarly low flux level during a different *XMM–Newton* observation is particularly low, i.e. in the range 12–18 per cent. Our inferred *XMM–Newton* fractional amplitude (∼8 per cent) is notably close to such range of values, it cannot be excluded that even a very small variation and decrement of the pulsed fraction (which is likely to happen) could have been sufficient to hamper its significant detection. In this respect, it is worth pointing out that when the ∼21 s coherent pulsations were discovered in the JEM-X data by using the Lomb–Scargle analysis (Sguera et al. 2007), the source was in a very bright outburst activity with a 3–10 keV L_x of $\sim 2 \times 10^{37}$ erg s^{-1}, i.e. almost four orders of magnitude brighter than the present *XMM–Newton* observation. Recently, Ducci et al. (2013) called into question such ∼21 s pulsation by reanalysing the JEM-X outburst data, however here we note that, among the others, the authors did not completely reproduce the same data analysis as in Sguera et al. (2007), e.g. the temporal range of their analysed outburst (MJD 53844.6–53846.0) is shorter (by ∼0.5 d) with respect to that analysed by Sguera et al. (2007). It is possible that in their timing analysis, Ducci et al. (2013) missed a significantly bright portion of the outburst activity as can be clearly seen from the corresponding light curve reported in Sguera et al. (2007).

Previous works (Rahoui & Chaty 2008; Romano et al. 2010) explained the observed X-ray outbursts from the SFXT IGR J18483−0311 by using the spherically symmetric clumpy wind scenario. Within this theoretical framework, it is generally assumed that the source goes into X-ray outburst activity preferentially during the periastron passage when orbiting inside regions of the supergiant wind characterized by a very high density of clumps much more massive than the background wind. In particular, Rahoui & Chaty (2008) found that a very eccentric orbit ($e = 0.4$–0.7) is strongly needed to explain the few days duration of some observed X-ray outbursts (as those reported in Sguera et al. 2007). In addition, assuming a large eccentricity of $e = 0.4$ Romano et al. (2009) explained the observed X-ray outbursts and their pronounced short time-scale variability in terms of accretion of single massive clumps composing the donor wind and having masses in the range 10^{18-20} g. We point out that the following new findings reported in the present study are hardly explainable by such spherically symmetric clumpy wind scenario: (i) both the significantly long X-ray outburst duration (at least ∼11 d) and the small variability factor (∼5) observed by *INTEGRAL* cannot be naturally explained by the accretion of single massive clumps embedded in a much less dense background wind. An unusually large number of clumps, incessantly accreted, would be required to continuously sustain the prolongated accretion of material for at least ∼11 d uninterruptedly (ii) part of the X-ray outburst activity was detected by *INTEGRAL* during the apastron approach, i.e. right when the neutron star is supposed to be incapable of accreting material because well outside the region of high-density clumps which is encountered only around periastron passage. The measured X-ray outburst luminosity, in the range (3–7) × 10^{35} erg s^{-1}, is too high to be explained in terms of accretion from the much less dense background wind (iii) the very low X-ray luminosity of ∼4 × 10^{33} erg s^{-1} was measured by *XMM–Newton* during the approach of the periastron passage when it is normally expected that the source goes into X-ray outburst. This missing activity is usually explained in term of extremely varying stellar wind environment (e.g. density and number of clumps) as probed by the neutron star on short orbital period time-scale (∼18.5 d in our specific case), which is somehow very difficult to accommodate and explain. On the contrary, the newly reported results have less shortcomings if explained within the quasi-spherical settling accretion model. In fact, (i) the low X-ray luminosity measured by *XMM–Newton* is well below the critical value of ∼3 × 10^{35} erg s^{-1}, this means that the source was inhabiting the radiatively cooled regime which allows only very low accretion rate on to the neutron star and so low L_x values, independently from the orbital phases of the system (ii) the outburst X-ray luminosity measured by *INTEGRAL* is above the critical value ∼3 × 10^{35} erg s^{-1}, and so the source was inhabiting the Compton cooling dominated regime which allows higher accretion rate on to the neutron star leading to the production of moderately bright flares with $L_x \leq 10^{36}$ erg s^{-1} as predicted by Shakura et al. (2014). The transition between the two regimes may be due to a switch in the X-ray beam pattern in response to a change in the optical depth in the accretion column with varying luminosity (Shakura et al. 2012, 2013). The triggering for the switch may be simply due to even very small and modest changes of the local wind velocity and density values, a condition very likely satisfied in a moderately clumpy wind scenario which realistically invoke smaller and lighter clumps, not necessarily very massive and large clumps as in the classical spherically symmetric clumpy wind scenario. Notably, the conditions for the transition are independent from the orbital phases of the system and so are not necessarily linked to periastron or apastron passages.

We note that the peculiar place occupied by the source in the Corbet diagram, lying close to the typical location of the Be HMXBs, lead Liu, Chaty & Yan (2011) to suggest that IGR J18483−0311 could be the descendant of a Be HMXB system. Liu et al. (2011) discuss this system as a source that is presently a wind-fed system, but it is tempting to suggest, given the longer outburst we discovered, that a variability in the donor wind conditions could have triggered the temporary formation of an accretion disc near the periastron passage, sustaining an unusually longer outburst due to the longer viscous disc time-scale. Variable wind conditions at the neutron star orbit could have been due to the crossing of a higher density large-scale wind variable structure similar to the spiral structures/shells discussed by Lobel & Blomme (2008). The different wind properties could have played a role in triggering an enhanced and longer accretion phase also within the quasi-spherical wind accretion scenario. We note that also another SGXB accreting pulsar with a peculiar location in the Corbet diagram, OAO1657−415, has been suggested to sometime undergo disc accretion phases, given its long-term secular spin-up of its pulsar (Mason et al. 2009). Interestingly enough, also OAO1657−415 has been suggested to be an SGXB evolved from a Be HMXB (Liu, Li & Yan 2010). Unfortunately, we cannot say anything conclusive about this scenario, given the lack of a long-term history of the IGRJ18483−0311 spin period derivative.

The newly discovered and unusually long X-ray activity observed from the SFXT IGR J18483−0311 represents a departure from the nominal behaviour of classical SFXTs with their much shorter outbursts and it adds a further extreme characteristic to the already extreme SFXT IGR J18483−0311. Further *INTEGRAL* studies on the classical SFXTs searching for similarly unusually long X-ray outbursts are needed to understand if the reported peculiar characteristic observed from IGRJ18483−0311 is exceptional or not among the class of SFXTs.

ACKNOWLEDGEMENTS

We thank an anonymous referee for useful comments which improved the quality of the paper.

REFERENCES

Bozzo E., Falanga M., Stella L., 2008, ApJ, 683, 1031
Bozzo E., Stella L., Ferrigno C., Giunta A., Falanga M., Campana S., Israel G., Leyder J. C., 2010, A&A, 519, 6
Chernyakova M., Lutovinov A., Capitanio F., 2003, Astron. Telegram, 157
Drave S. P., Bird A. J., Sidoli L., Sguera V., McBride V. A., Hill A. B., Bazzano A., Goossens M. E., 2013, MNRAS, 433, 528
Drave S. P., Bird A. J., Sidoli L., Sguera V., Bazzano A., Hill A. B., Goossens M. E., 2014, MNRAS, 439, 2175
Ducci L., Sidoli L., Mereghetti S., 2009, MNRAS, 398, 2152
Ducci L., Doroshenko V., Sasaki M., Santangelo A., Esposito P., Romano P., Vercellone S., 2013, A&A, 559, 135
Ducci L., Doroshenko V., Romano P., Santangelo A., Sasaki M., 2014, A&A, 568, 76
Giunta A. et al., 2009, MNRAS, 399, 744
Grebenev S. A., Sunyaev R. A., 2007, Astron. Lett., 33, 149
Lebrun F. et al., 2003, A&A, 411, L141
Levine A. M., Corbet R., 2006, Astron. Telegram, 940
Levine A. M., Bradt H. V., Chakrabarty D., Corbet R. H. D., Harris R. J., 2011, ApJS, 196, 6
Liu Q. Z., Li H., Yan J., 2010, Sci. China Phys. Mech. Astron., 53, 130
Liu Q. Z., Chaty S., Yan J. Z., 2011, MNRAS, 415, 3349
Lobel A., Blomme R., 2008, ApJ, 678, 408
Lorenzo J., Negueruela I., Castro N., Norton A. J., Vilardell F., Herrero A., 2014, A&A, 562, A18
Luna G. J. M., Sokoloski J. L., 2007, ApJ, 671, 741
Lund N. et al., 2003, A&A, 411, L231
Mason A. B., Clark J. S., Norton A. J., Negueruela I., Roche P., 2009, A&A, 505, 281
Negueruela I., Smith D., Reig P., Chaty S., Torrejón J. M., 2006, in Wilson A., ed., ESA SP-604: X-ray Universe 2005. ESA, Noordwijk, p. 165

Negueruela I., Torrejon J. M., Reig P., Ribó M., Smith D. M., 2008, in Bandyopadhyay R. M., Wachter S., Gelino D., Gelino C. R., eds, AIP Conf. Proc. Vol. 1010, A Population Explosion: The Nature & Evolution of X-ray Binaries in Diverse Environments, Am. Inst. Phys., New York, p. 252
Nelson R. W., Salpeter E. E., Wasserman I., 1993, ApJ, 418, 874
Nelson R. W., Wang J. C. L., Salpeter E. E., Wasserman I., 1995, ApJ, 438, L99
Oskinova L. M., Feldmeier A., Kretschmar P., 2012, MNRAS, 421, 2820
Paizis A., Sidoli L., 2014, MNRAS, 439, 3439
Press W. H., Rybicki G. B., 1989, ApJ, 338, 277
Rahoui F., Chaty S., 2008, A&A, 492, 163
Romano P., Sidoli L., Cusumano G., Vercellone S., Mangano V., Krimm H. A., 2009, ApJ, 696, 2068
Romano P. et al., 2010, MNRAS, 401, 1564
Scargle J. D., 1982, ApJ, 263, 835
Sguera V. et al., 2005, A&A, 444, 221
Sguera V. et al., 2006, ApJ, 646, 452
Sguera V. et al., 2007, A&A, 467, 249
Sguera V., Ducci L., Sidoli L., Bazzano A., Bassani L., 2010, MNRAS, 402L, 49
Sguera V., Drave S. P., Sidoli L., Masetti N., Landi R., Bird A. J., Bazzano A., 2013, A&A, 556, 27
Shakura N., Postnov K., Kochetkova A., Hjalmarsdotter L., 2012, MNRAS, 420, 216
Shakura, Postnov K., Hjalmarsdotter L., 2013, MNRAS, 428, 670
Shakura, Postnov K., Sidoli L., Paizis A., 2014, MNRAS, 442, 2325
Sidoli L., Romano P., Mereghetti S., Paizis A., Vercellone S., Mangano V., Götz D., 2007, A&A, 476, 1307
Sidoli L. et al., 2008, ApJ, 687, 1230
Sidoli L., Esposito P., Ducci L., 2010, MNRAS, 409, 611
Struder L. et al., 2001, A&A, 365, L18
Torrejon J. M., Negueruela I., Smith D. M., Harrison T. E., 2010, A&A, 510, 61
Turner M. J. L. et al., 2001, A&A, 365, L27
Ubertini P. et al., 2003, A&A, 411, L131
Walter R., Zurita H. J., 2007, A&A, 476, 335
Winkler C. et al., 2003, A&A, 411, L1

This paper has been typeset from a TEX/LATEX file prepared by the author.